Matrix isolation technique for the study of some factors affecting the partitioning of trace elements.

Joseph M. Grzybowski and Ralph O. Allen*
Department of Chemistry
University of Virginia
Charlottesville, VA 22901

ABSTRACT

Some of the factors that affect the preferred positions of cations in ionic solid solutions were investigated utilizing vibrational spectroscopy. Solid solutions of the sulfate and chromate ions codoped with La^{+3} and Ca^{+2} in a KBr host lattice were examined as a function of the polyvalent cation concentration. The cation-anion pairing process was found to be random for Ca^{+2} whereas the formation of La^{+3}-SO_4^{-2} ion pairs with a C_{2v} bonding geometry is highly preferential to any type of La^{+3}-CrO_4^{-2} ion pair formation. The relative populations of ion pair site configurations are discussed in terms of an energy-entropy competition model which can be applied to the partition of trace elements during magmatic processes.

*Author to whom correspondence should be addressed.

(NASA-CR-139618) MATRIX ISOLATION TECHNIQUE FOR THE STUDY OF SOME FACTORS AFFECTING THE PARTITIONING OF TRACE ELEMENTS (Virginia Univ.) 26 p HC $4.50 CSCL 07D G3/06

N74-31593

Unclas 46719

INTRODUCTION

Trace element partition coefficients between silicate melts and crystallizing minerals have been measured and found useful as a measure of magmatic differentiation. It has become clear that the partitioning of trace elements into minerals depends upon several atomic and crystal chemical factors. In some cases the ionic size is the most important factor as suggested by Goldschmidt (1937)(eg Onuma et al. 1968), while in others ionization potentials (eg Ringwood, 1955), or the stabilization energy of crystal-fields (eg Burns and Fyfe, 1964) are the dominant factors. Burns and Fyfe (1966) among others have treated the substitution of trace elements in a solid solution in terms of the thermodynamics of the equilibrium: $X^+(magma) + Y^+Z^-(crystal) \rightleftarrows X^+Z^-(crystal) + Y^+(liquid)$ Whittaker (1967), who made similar considerations, took a more atomistic approach to the problem and concluded that the difference between the internal energies of the substituting trace element (X^+) and the major cation (Y^+) which it replaces must be considered in both the liquid and the crystalline environment. The partitioning of cations in the solid phase can be studied for natural systems. For instance, the ordering of the major cations over two distinct octahedral sites in olivine has been studied using infrared spectroscopy (Huggins, 1973). In natural minerals vibrational bands of anions are broadened by resonance coupling between neighboring identical anions. These broad bands prevent the direct observation of the effects of trace concentrations of cations on the vibrational spectrum. In ionic solid solutions where anions are isolated from

each other by the host matrix, the vibrational bands are narrow and splittings due to the orientation of the cation can be observed.

In order to study the various factors that influence which cations will go into a particular lattice site or which site will be preferred by a cation, a matrix-isolation technique has been used. A solid solution is formed with anions of the form XY_4^{-2}(eg SO_4^{-2}, CrO_4^{-2}) and an alkali halide (eg KBr). When multiply charged cations are added to the melt they pair with the divalent anions to achieve charge neutrality. The position the cation assumes in the lattice is affected by the same factors that are important in determining the lattice positions and concentrations of trace cations in silicate systems. Although tne anions reported here are not of great importance in rock forming minerals it shows the value of the technique which can be applied to other anions.

The cubic structure possessed by several alkali halides can be described in terms of two interpenetrating face-centered cubic lattices (one containing the alkali ions and the other containing the halide ions) and the symmetry of each occupied lattice site is Oh. The relative coordinates of the two sublattices can be expressed as (0, 0, 0) and 1/2, 0, 0), respectively.

This alkali halide cell (Figure 1, without M^{+m}-XY_4^{-n} substitution and association of an M^{+m} cation) determines the bonding geometry and, therefore, the site symmetry of the ion pair. In terms of the Atypical Cell model, the XY_4^{-n} ion is substituted at a halide ion lattice site

and rigidly oriented as illustrated in the figure. An interstitial type of solid solution is expected to be less favorable owing to steric hindrance, which is caused by the large size of the XY_4^{-n} ions. The validity of this assumption, relative to any type of random orientation of the XY_4^{-n} ion in the cell, is confirmed by the polarized Raman spectra obtained with a solid solution of this type.. (Grzybowski and Khanna, 1974).

The M^{+m} cation, which becomes associated with such a complex anion, may either substitute for one of the alkali ions in the lattice or find some interstitial position. Occupation of the interstitial lattice positions becomes increasingly more improbable as the cation diameter increases. Therefore, the substitutional M^{+m} lattice positions deserve the greatest consideration with regard to their effects on the vibrational spectrum of the ion pair. Lattice vacancies are formed in the alkali halide host lattice to maintain overall electrical neutrality when the dopants are not of identical, but opposite charge and must also be considered.

The ion pair bonding geometry can be determined by examining the spectroscopically observed vibrational band pattern of the internal modes of the complex anion, XY_4^{-n}. The triply degenerate assymetric stretch mode of the XY_4^{-n} ion is very intense in the infrared, and is quite sensitive to inhomogeneities in the localized crystal field produced about the anion by the M^{+m} cation and/or associated lattice vacancies. Lattice vacancies may occur at a sufficient distance from the ion pair so as not to affect

the local crystal field about the ion pair. The bonding geometry of the ion pair and the relative separation of the two ions can be determined by utilization of a group theoretical analysis of the vibrational spectrum of the XY_4^{-n} ion. (eg Decius et al. (1963), Miller et al. (1971), Grzybowski and Khanna (1974)).

If the XY_4^{-n} anion is oriented as above (Figure 1), the M^{+m} cation can substitute for an alkali ion at any one of three distinct sets of non-equivalent near neighbor lattice sites. These sites are labeled (a), (b), and (c), resulting in ion pair site symmetries of $C_{3v}(a)$, $C_{3v}(b)$, and C_{2v}, respectively, The number of infrared active bands resulting from a splitting of the degeneracy of the anion's assymetric stretch mode for each of these configurations is 2, 2, and 3 respectively. Associated lattice vacancies may further modify the site symmetry and the observed spectrum but will not necessarily modify substantially the bonding geometry of the M^{+m}-XY_4^{-n} ion pair. The case in which there is no pairing between the M^{+m} and XY_4^{-n} ions is unique in that there is no splitting of the degeneracy of the assymetric stretch mode of the anion in the infrared spectrum.

EXPERIMENTAL METHOD

The solid solution samples were grown as single crystals from the melt by a modified Bridgemann (1925) technique.

The samples were prepared with about 8 grams of KBr and an initial doping concentration of K_2SO_4 and/or K_2CrO_4 of 0.03 precent by mole. The initial doping concentration of La^{+3} or Ca^{+2} (in the form of $LaBr_3$ or $CaBr_2$) was varied relative to the fixed total divalent anion concentration. Each sample was then placed in a tapered bottom quartz sample tube which was placed in a modified Bridgemann furnace to allow the sample to melt. The tube was then lowered through a continuous temperature gradient such that the sample temperature was lowered from about 800°C to 25°C over a period of three days. The single crystals obtained in this way were visibly transparent throughout all but the uppermost eighth of the crystal. The uppermost section of each crystal was visibly turbid and contained large occlusions of the dopants and, therefore, was not used in the analysis. This indicates that the concentration of the dopants in solid solution are much lower than the initial doping concentrations. The transparent crystal section was cut into samples approsimately 1.5cm x 7mm x 7mm in dimension. The infrared spectrum of each sample was recorded at room temperature with a Perkin-Elmer Model 521 Infrared spectrophotometer. The spectra were recorded between 1300 and 800cm^{-1} which allowed examination of the two fundamental stretching modes of the SO_4^{-2} and CrO_4^{-2} ions.

The initial doping concentration of the La^{+3} (or Ca^{+2}) ion relative to an initial doping concentration of 0.03 mole percent for the CrO_4^{-2} and SO_4^{-2} ions is described in terms of a doping ratio of the form (M^{+m}:SO_4^{-2}:CrO_4^{-2}). This indicates the total number of M^{+m} cations available per single anion (SO_4^{-2} or CrO_4^{-2}). An overall cation to anion ratio

$(M^{+m}:[XY_4^{-n}]total)_T$ is also presented which directly gives the number of M^{+m} cations available per XY_4^{-n} anion without distinction between different anions.

RESULTS

The relative concentrations of mixed solid solutions of the type M^{+m}-SO_4^{-2}-CrO_4^{-2}/KBr were studied to obtain information on the preferential bonding properties of the M^{+m} cation for either anion.

The first mixed solid solution system examined was Ca^{+2}-SO_4^{-2}-CrO_4^{-2}/KBr. The infrared spectra of singular solid solutions of Ca^{+2}-SO_4^{-2}/KBr and of Ca^{+2}-CrO_4^{-2}/KBr have been thoroughly examined by Decius et al. (1963) and by Miller et al. (1971), respectively. In the mixed solid solution (SO_4^{-2} and CrO_4^{-2}) examined here, the results were a superposition of those of the singular solid solutions. With either anion the dominant bonding geometry has the anion paired with the Ca^{+2} cation in the C_{2v} position. Spectroscopically, this is indicated by the presence of the intense bands at 1182, 1150 and 1081cm^{-1} for the SO_4^{-2} ion and at 932, 920, and 876cm^{-1} for the CrO_4^{-2} ion. The absorption band due to the assymetric stretch mode of ($Td(F_2)$) each isolated anion (without Ca^{+2} association) also appears with appreciable intensity at about 1130cm^{-1} for the SO_4^{-2} ion and about 904cm^{-1} for the CrO_4^{-2} ion. The appearance of these bands strongly indicate that not all M^{+m} cations need necessarily be bonded to an XY_4^{-n} anion even if m=n. Perhaps the most important point to be made

upon examination of the Ca^{+2}-SO_4^{-2}-CrO_4^{-2}/KBr solid solution system is that there is no preferential bonding or association of the Ca^{+2} cation with either of the two anions investigated. This is apparent in the simultaneous appearance and growth of the very narrow (approximately $5cm^{-1}$ halfwidth) absorption bands due to the presence of either anion at random bonding to a Ca^{+2} cation as the dopant ratio increases from (0:1:1) to (4:1:1).

In order to determine the feasability of using mixed solid solutions to characterize any preferential bonding properties of a Rare Earth cation for a particular anion, the solid solution series La^{+3}-SO_4^{-2}-CrO_4^{-2}/KBr was examined. The singular solid solutions of La^{+3}-SO_4^{-2}/KBr and La^{+3}-CrO_4^{-2}/KBr were examined as references. Figure 4 gives the observed spectra for the La^{+3}-SO_4^{-2}/KBr solid solution system over the concentration range (0:1) to (2:1). The sample with a doping ratio of (0:1) has no La^{+3} to ion pair with the SO_4^{-2} ion. Therefore, the two observed broad bands at 1115 and $1150cm^{-1}$ are due to aggregate formation of the SO_4^{-2} ions in the host lattice and/or anion-lattice vacancy pairing (type A bands). As the dopant ratio is increased to (0.5:1), several new bands appear in the spectrum. These bands are observed at about 1180, 1155, and $1085cm^{-1}$ (type B bands) and are consistent with an ion pair bonding geometry of C_{2v}. A further dopant ratio increase to (1:1) produces a relative intensity increase in the type B bands relative to the type A bands. A further increase in the La^{+3} cation concentration resulting in a dopant ratio of (2:1) produces variations in the spectrum that do not completely

follow the trend established by the less concentrated members of the series. As is illustrated in Figure 4 by the two different spectra obtained from different sections of the most concentrated crystal, the bands due to the C_{2v} ion pair bonding geometry vary in intensity relative to the anion-lattice vacancy pairing bands. Apparently, a very high La^{+3} concentration induces the formation of lattice vacancies and/or aggregate formation. The shoulders that appear on the type A bands are apparently the result of a pairing of the SO_4^{-2} to at least one La^{+3} cation and possibly one or more lattice vacancies to achieve charge balance.

The infrared spectra of La^{+3}-CrO_4^{-2}/KBr solid solutions are reproduced in Figure 5. Beginning with a dopant ratio of (0:1) four bands appear in the spectrum. The two very intense bands at about 920 and 890cm^{-1} (type C bands) are directly analogous to the type A bands of the La^{+3}-SO_4^{-2}/KBr solid solution system. The weak shoulders at 836 and 868cm^{-1} on the type C bands are due to pairing of the CrO_4^{-2} ion with a near neighbor lattice vacancy or due to contamination by cations at concentrations as low as several PPM. Upon increasing the dopant ratio to (0.5:1), three new bands are evident. The type C bands are still dominant, however, the strong band (type E band) at about 900cm^{-1} is due to the triply degenerate assymetric stretch mode of the CrO_4^{-2} ion isolated within the KBr host lattice. The low intensity bands (type D bands) that appear at 933 and 876cm^{-1} are two of the three bands expected for the C_{2v} ion pair bonding geometry. The third band (919cm^{-1}) in this group falls under

the envelope of the intense 920cm^{-1} type C band. The infrared spectrum of the (1:1) dopant ratio sample clearly illustrates that all three type D bands are present and increasing in intensity relative to the type C and type E bands. A further dopant ratio increase to (2:1) results in a further increase in the relative intensities of these bands relative to the type C and type E bands. Just as with the most concentrated La^{+3}-SO_4^{-2}/KBr sample, the relative intensities between each band type varied with the sample section which was used to obtain the spectrum. This observation lends further evidence in favor of the assumption that high La^{+3} concentrations induce the presence of high concentrations of lattice vacancies in order to achieve overall charge neutrality.

The infrared spectra of the La^{+3}-SO_4^{-2}-CrO_4^{-2}/KBr mixed solid solution system are illustrated in Figure 6. This solid solution system displays dramatic changes in the infrared spectra of the samples doped with varying initial concentrations of La^{+3}. The infrared spectrum of the mixed solid solution with a doping ratio of (0:1:1) displays the type A bands from the La^{+3}-SO_4^{-2}/KBr solid solution series, and the type C bands from the analogous CrO_4^{-2} solid solution series. However, the type A and type C bands in this series are more assymetric and broader than the corresponding bands in the singular solid solutions, indicating the presence of unresolved bands in these regions. Increasing the dopant ratio to (0.5:1:1) should give rise to the type B and type D bands of the SO_4^{-2} and CrO_4^{-2} ions, if as in the case of Ca^{+2} there is no preferential association of the La^{+3} ion with either of the two anions.

The type A and type B bands of the SO_4^{-2} ion appear as do the type C bands of the CrO_4^{-2} ion. The type D bands corresponding to a C_{2v} bonding geometry of the La^{+3}-CrO_4^{-2} ion pair are conspicuously absent from the spectrum, indicating preferential bonding of the La^{+3} ion with the SO_4^{-2} ion in solid solution with the C_{2v} ion pair bonding geometry. Similar results are obtained with a doping ratio of (1:1:1), the main difference being an increase in the type B bands relative to the type A bands for the SO_4^{-2} ion. The type D bands for the CrO_4^{-2} ion are still absent from the spectrum and the type C bands of the CrO_4^{-2} ion decrease relative to the type A bands of the SO_4^{-2} ion. This is interpreted as an increased tendency to reject the CrO_4^{-2} ion from the solid solution as the La^{+3} ion concentration is increased. The most dramatic changes in the infrared spectra of this system occur upon increasing the dopant ratio to (2:1:1). As with the singular solid solutions, high concentrations of La^{+3} tend to produce changes that depend upon which crystal section was used to obtain the infrared spectrum. These changes, however, are minor and are only related to changes in the relative intensities of the observed solid solution bands. The two extreme cases in the observed spectra are reproduced in the figure. One important feature is that both the D and C bands of the CrO_4^{-2} ion are absent from the spectra which suggests that the CrO_4^{-2} ion is not in solid solution. In fact visible occlusions of the yellow CrO_4^{-2} ion were found in one section of the crystal grown at this high La^{+3} concentration.

Another feature is the set of three assymetrically spaced bands at 1214, 1165, and 1031cm^{-1} (type F bands) in the SO_4^{-2} assymetric stretch region of the spectrum. The type F bands are consistent with the simultaneous pairing of the SO_4^{-2} ion with one La^{+3} cation and an alkali ion lattice vacancy in the opposing face centered lattice site of the Atypical Cell (Figure 1). The band at 1214cm^{-1} also appeared at very low intensity in the singular (1:1) La^{+3}-SO_4^{-2}/KBr solid solution (the other two type F bands were evidently lost in the background). As with the samples possessing a low dopant ratio, the type A and type B bands appear. The major difference being their drastically varying intensities relative to the type F bands which depend directly upon the sample section that was used to obtain the infrared spectr Also, the weak band that appears at 966cm^{-1} is the totally symmetric stretch mode for the SO_4^{-2} ion and is associated with the type F bands. Lastly, an increase in the dopant ratio to (4:1:1) yields spectra that show the same general features and variability as those obtained for the system having a dopant ratio of (2:1:1).

CONCLUSIONS

These experiments prove this technique to be valuable in studying ion pairs in solid solutions. Vibrational spectroscopy indicates that cations at trace levels occupy lattice sites in the crystal rather than at interstitial positions or as separate grains. Even when there is a charge imbalance in the ion pair formed, the multivalent cation still occupies a lattice site and the imbalance is alleviated by lattice vacancies. Both La^{+3} (ionic radius 1.15 Å) and Ca^{+2} (ionic radius .99 Å) fit into the same lattice site (C_{2v}) relative to either anion. However, when both anions are present the two cations behave in very different manners. The Ca^{+2} goes into the solid solution in a random fashion with both anions while the La^{+3} is more selective. The pairing of La^{+3} with the SO_4^{-2} is so strong that CrO_4^{-2} is excluded from the lattice even when excess La^{+3} is present. This is a very clear demonstration that there are influences other than ionic size or charge involved in the formation of ion pairs in solid solution. It is possible by this technique to observe the competition between different cations for different anions with which to pair. This is analogous to the case of the selective substitution by trace cations in different lattice sites of rock forming minerals. In minerals and the solid solutions described in this paper anions containing oxygen interact with cations, and in many cases the bonding is primarily ionic. It has been shown (Grzybowski, 1972) that in this type of ionic solid solution the cations can diffuse to

the most energetically favorable lattice positions. The anions, on the other hand, do not diffuse after crystallization so that the isolation of the complex anions from each other in the solid solution must occur during crystallization at the solid-liquid interface. In the case of the La^{+3}-SO_4^{-2}-CrO_4^{-2}/KBr solid solution the absence of the assymetric stretch mode of the isolated CrO_4^{-2} ion indicates that this anion does not enter the lattice at all rather than being a case of La^{+3} diffusing away from the CrO_4^{-2} after crystallization. This indicates that La^{+3}-SO_4^{-2} forms a much more stable ion pair than La^{+3}-CrO_4^{-2} during the formation of the solid solution. Although further study is required, this can be qualitatively understood in terms of the Hard and Soft Acid- Base concept discussed by Pearson (1973). The La^{+3} is a very "hard" cation (harder than Ca^{+2}), the SO_4^{-2} is a "harder" anion than the CrO_4^{-2} ("hard" indicating relatively unpolarizable ions). The hardest anions and cations form the strongest ion pair (La^{+3}-SO_4^{-2}) while those involving Ca^{+2} or CrO_4^{-2} are not as strong.

The other important parameter which can be studied by this technique is the lattice position filled by the cations. The relative stabilities or these sites are determined by an energy-entropy competition. Thermodynamic considerations require a minimization of the Helmholtz free energy $A=E_{int}-TS$ (where E_{int} is the internal energy of the solid solution, T the temperature, and S is the entropy of the solid solution). At low temperatures the energy term is dominant and those site configurations which possess the largest negative E_{int} should be most stable.

As a first approximation, the energy of formation of a particular site configuration can be considered in terms of an electrostatic charge compensation. The entropy is directly related to the number of identical cation lattice sites (degeneracy) which can produce the particular ion pair site configuration.

In the solid solutions studied possible positions of the cations are limited by the crystal to lattice positions. (The positions of trace element cations are also confined to a limited number of sites within the lattice of crystallizing minerals). Some cation lattice positions are more effective in compensating for the anion charge than others. One extreme case is for the cations to assume the C_{2v} position as both La^{+3} and Ca^{+2} did. This lattice position places the cation near two oxygen atoms of the anion and is the most effective means of compensating for the excess charge. This can be most readily understood if the two ions are considered as point charges separated by a distance r_i (the ion pair bond length) within a non-interacting medium (the KBr host lattice). The potential energy becomes more negative as r_i decreases ($Ei \alpha \frac{-1}{r_i}$). The energy (Ei) is, therefore, the most negative for the C_{2v} ion pair configuration where r_i is the smallest under the constraints imposed by the lattice. There are six of these C_{2v} cation positions (equivalent) around the complex anion. Thus for this position the energy term is large and negative and is dominant when compared to the entropy term (degeneracy). There are however a series of sites

that the cation can occupy at greater distances from the anion. The ion pairing energy for these sites become substantially smaller as the anion-cation separation becomes larger. The local charge compensation is minimal in these configurations. The resulting site symmetry is Td and the degeneracy is large in that there are many equivalent sites. Thus for these lattice positions, the entropy term is dominant and at higher temperatures this site should be most stable. Earlier results on similar solid solutions suggest that the C_{2v} sites present at room temperature can be transformed to Td configurations and the intermediate C_{3v} configurations by intense heat treatment (Grzybowski and Khanna, 1974). After standing at room temperature for 8 months the cations in the heat treated sample returned to the energetically favorable C_{2v} lattice positions.

In addition to La^{+3} and Ca^{+2} most other cations studied to date assumed the C_{2v} lattice position at low (room) temperatures, but many show a definite population of other sites as well and in some cases a dominance of C_{3v} sites. A qualitative description of the different sites in terms of the number of cation-anion bonds, effectiveness of charge balance and degeneracy of the sites is given in Table 1. Although the exact energies of the various site configurations have not been calculated, the relative energy levels have been determined on the basis of these studies. In addition to the energy of formation of the individual ion-pair site configurations, there are sublevels (especiall

for the La^{+3} case) associated with the formation of various lattice vacancies. A schematic energy level diagram is shown in Figure 7. The exact energy level of any one site or the energy differences between sites will change for different ion-pairs as discussed below. The fraction of the cations in each different site can be described in terms of a Boltzmann distribution law of the form $\frac{Ni}{N} = \frac{di}{f} e^{-Ei/kT}$ where Ni is the number of cations in lattice site i with internal energy Ei and a degeneracy di. N is the total number of cations in the solid solution, Ni/N is a partition coefficient and f is the sum over all available lattice sites ($f = \sum_i di\ e^{-Ei/kt}$). Schematically this type of distribution is shown for two different temperatures in Figure 7. This shift in the distribution has been used to explain the changes observed in the vibrational spectra of these solid solutions with heat treatment (Grzybowski and Khanna, 1974).

The important aspect of this type of consideration to geochemical problems is that in these simple solid solutions the affects of various crystallographic and atomic parameters can be studied and quantified. Since the energy and entropy of site occupation changes when a trace element substitutes for a major cation in the lattice of a growing mineral crystal, the factors which affect these changes must be quantified in order to predict distribution coefficients. Although we are presently unable to give quantitative results, the behavior of different cations and anions in ionic solid solutions enable us to make some comments on the general trends. It is found that hard cations (small and only weakly

polarizable) interact more strongly (lowering the energy of ion-pair formation) with hard anions. Cations which are more easily polarized (soft) tend to form more covalent type bonds with the softer anions. For the case of Ca^{+2} and Cd^{+2} which have nearly the same ionic radii, the electronic polarizability of the Cd^{+2} (1.8 $\AA^3$) is greater than that for Ca^{+2} (1.1 $\AA^3$). While the C_{2v} position is dominant for Ca^{+2} with the soft CrO_4^{-2} anion, the C_{3v} sites are appreciably populated by the Cd^{+2}. This can be interpreted as a shift of the ion-pair energy levels (Ei) to lower energies for the softer Cd^{+2}-CrO_4^{-2} ion pair. Since the total energy of the system at any given temperature will be the same, there will be an increase in the population of the sites above C_{2v}.

The polarizability of the anion and the lattice are also important in these systems (the analogous situation in minerals would be the polarizability of various silicate lattices). In most of the studies made to date the cations have been harder than any of the anions. A tendency has been observed that the softer the anion, the more dominant the C_{2v} site becomes. For instance, Pb^{+2} shows appreciable tendency to occupy the C_{3v} sites in solid solutions of the relatively hard BeF_4^{-2} ion which is about the same size as the CrO_4^{-2} anion for which the C_{2v} site is dominant. The harder the anion pairing with the energy of relatively hard cations the lower ion pair formation becomes, thus more cations occupy some of the more abundant sites which are not as effective in yielding local charge balance (such as the C_{3v} sites). Solid solutions were prepared in KCl, KBr, and KI (which increase in size

and polarizability) to see what role the lattice played in the population of sites. Although it isn't possible to separate the size and polarizability effects, the KI lattice was observed to stabilize the C_{2v} site relative to the C_{3v} site and it makes lattice defects (K^+ ions missing) more probable. For the case of Cd^{+2}-CrO_4^{-2} in KCl, the C_{3v} sites become occupied as opposed to the C_{2v} sites observed in KBr. The KBr lattice is more polarizable than the CrO_4^{-2} anion, so the relatively hard Cd^{+2} cation forms a fairly strong ion pair with the CrO_4^{-2} ion. On the other hand, when the polarizability of the lattice around the site becomes smaller the hard cation begins to interact more strongly with the lattice. This favors the C_{3v} site where the cation can interact strongly with both the anion and the lattice.

Thus the effects of the polarizability of the ions and the lattice sites can be visualized in terms the rules set forth in the hard and soft acid- base concept (Pearson, 1973). The other important parameters are the size of the ions involved. The entropy will drive the cations to occupy the most degenerate sites. If the cation becomes too large relative to the size of a lattice site, a distortion of the lattice will occur increasing the ion-pair energy (Ei) of that configuration. This is in line with our observation that the larger cations occupy the C_{2v} sites while smaller ones have appreciable populations of the C_{3v} sites. An example would be the Cd^{+2} (ionic radius = .97 Å) and Sr^{+2} (ionic radius = 1.13 Å) with CrO_4^{-2} in the KBr lattice. The polarizabilities of the cations are about the same, but the smaller Cd^{+2} cations occupied

the C_{3v} sites (especially C_{3v}) versus the C_{2v} sites occupied more fully by the Sr^{+2}. A similar pattern of behavior is observed for the distribution coefficients of minerals with respect to the size of the cation which is going into a lattice position of some fixed size. Onuma et al. (1968) for instance, observed that the partition coefficients for the lanthanides which replace Ca^{+2} in the lattice of bronzite, decrease as the size of the lanthanide ion increases. In terms of the reasoning suggested above, this is due to an increase in the ion pair energy (Ei) due to the necessary lattice distortion. It might be anticipated that as the size of the anion increases the size of some of the lattice positions (C_{3v}^{a}) decrease while bringing the charge centers (oxygen atoms) closer to others (C_{3v}^{b} and C_{2v}) giving rise to stronger interactions between the ion-pair.

The rather crude models proposed can adequately explain the factors observed to affect the occupied sites of the cations in the ionic solid solutions studied. These same models also provide a way of rationalizing trace element partition coefficients. It should be possible in future studies to begin to quantify these factors so that they can be used to predict behavior in the more complex solid solutions found in nature.

FIGURE CAPTIONS

Figure 1: Schematic diagram of the cell utilized for interpretations in the Atypical Cell Model.

Figure 2: Room temperature infrared spectra of the Ca^{+2}-SO_4^{-2}-CrO_4^{-2}/KBr mixed solid solution system as a function of the Ca^{+2} ion concentration. The doping ratios are: a)(0:1:1), or $(0:2)_T$; b)(1:1:1); c)(2:1:1), or $(1:1)_T$; d)(4:1:1), or $(2:1)_T$.

Figure 3: Room temperature infrared spectra of the La^{+3}-SO_4^{-2}/KBr singular solid solution system as a function of the La^{+3} ion concentration. The doping ratios are: a)(0:1); b)(0.5:1); c)(1:1); d)(2:1).

Figure 4: Room temperature infrared spectra of the La^{+3}-CrO_4^{-2}/KBr singular solid solution system as a function of the La^{+3} ion concentration. The doping ratios are: a)(0:1); b)(0.5:1); c)(1:1); d)(2:1).

Figure 5: Room temperature infrared spectra of the La^{+3}-SO_4^{-2}-CrO_4^{-2}/KBr mixed solid solution system as a function of the La^{+3} ion concentration. The doping ratios are: a)(0:1:1), or $(0:2)_T$; b)(1:1:1); c)(2:1:1), or $(1:1)_T$; d)(4:1:1), or $(2:1)_T$.

Figure 6: Schematic energy level diagram (left) and the corresponding site population distribution function (right) for ionic solid solutions.

TABLE 1. The Statistics of the Multivalent Cation Distribution for the Major Site Configurations

Major Site Symmetry	Degeneracy of the Lattice Site for the Multivalent Cation	Number of Near Neighbor XY_4^{-2} Bonds	Effectiveness of Local Charge Compensation*
T_d	1000+	0	Very Poor
C_{2v}	6	2	Excellent
C_s	6 + vacancy	2	Good to Very Good
C_{3v}^b	4	1	Good
C_s^b	4 + vacancy	1	Good to Very Good
C_{3v}^a	4	3	Very Good

*As determined by considering only an electrostatic charge compensation interaction.

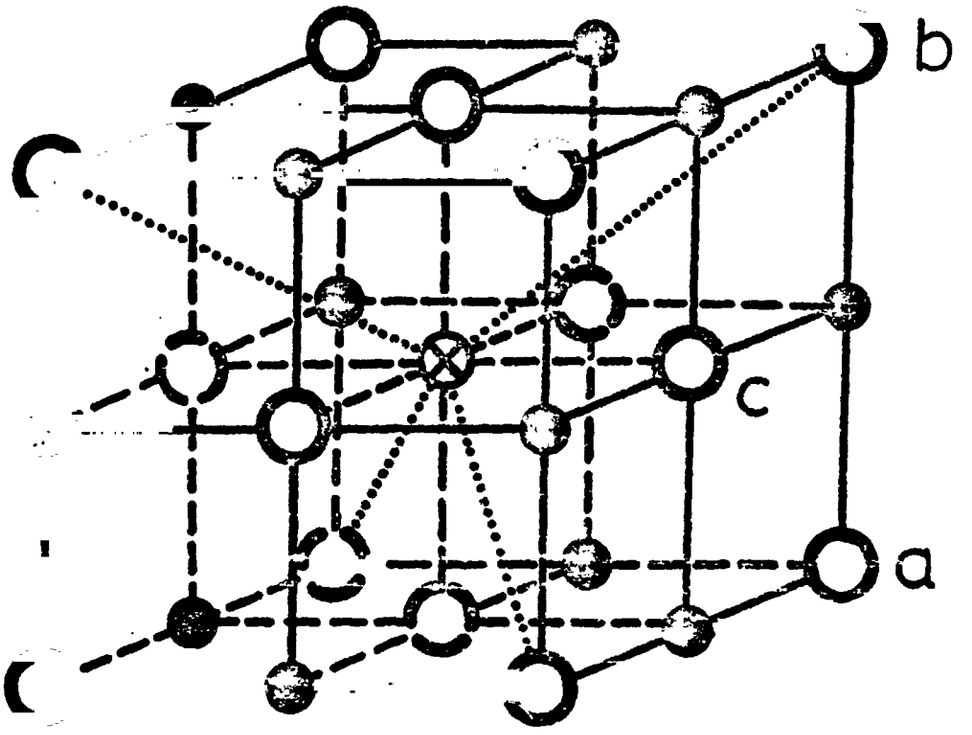

FIGURE 1: SCHEMATIC DIAGRAM OF THE CELL UTILIZED FOR INTERPRETATIONS IN THE ATYPICAL CELL MODEL

○ indicates a cation lattice site

● indicates an anion lattice site

⊗ indicates substitution of XY_4^{-2} at an anion lattice site with the relative orientations of the four X-Y bonds indicated by the dotted lines

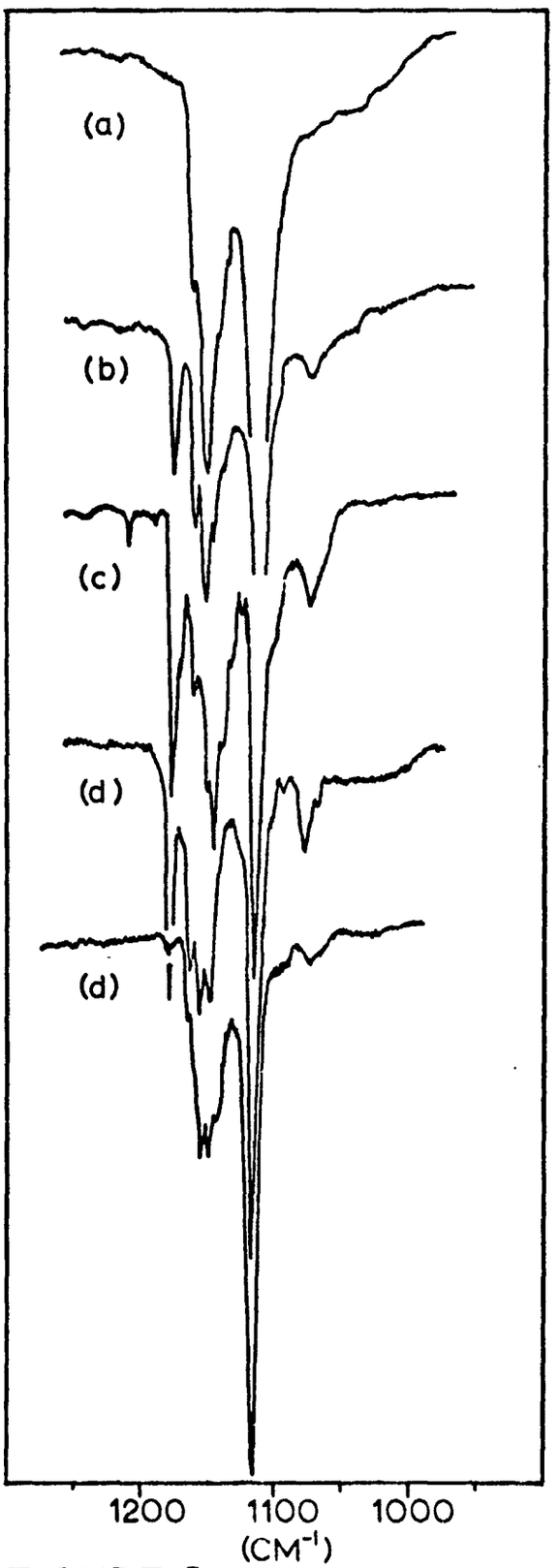

FIGURE 3

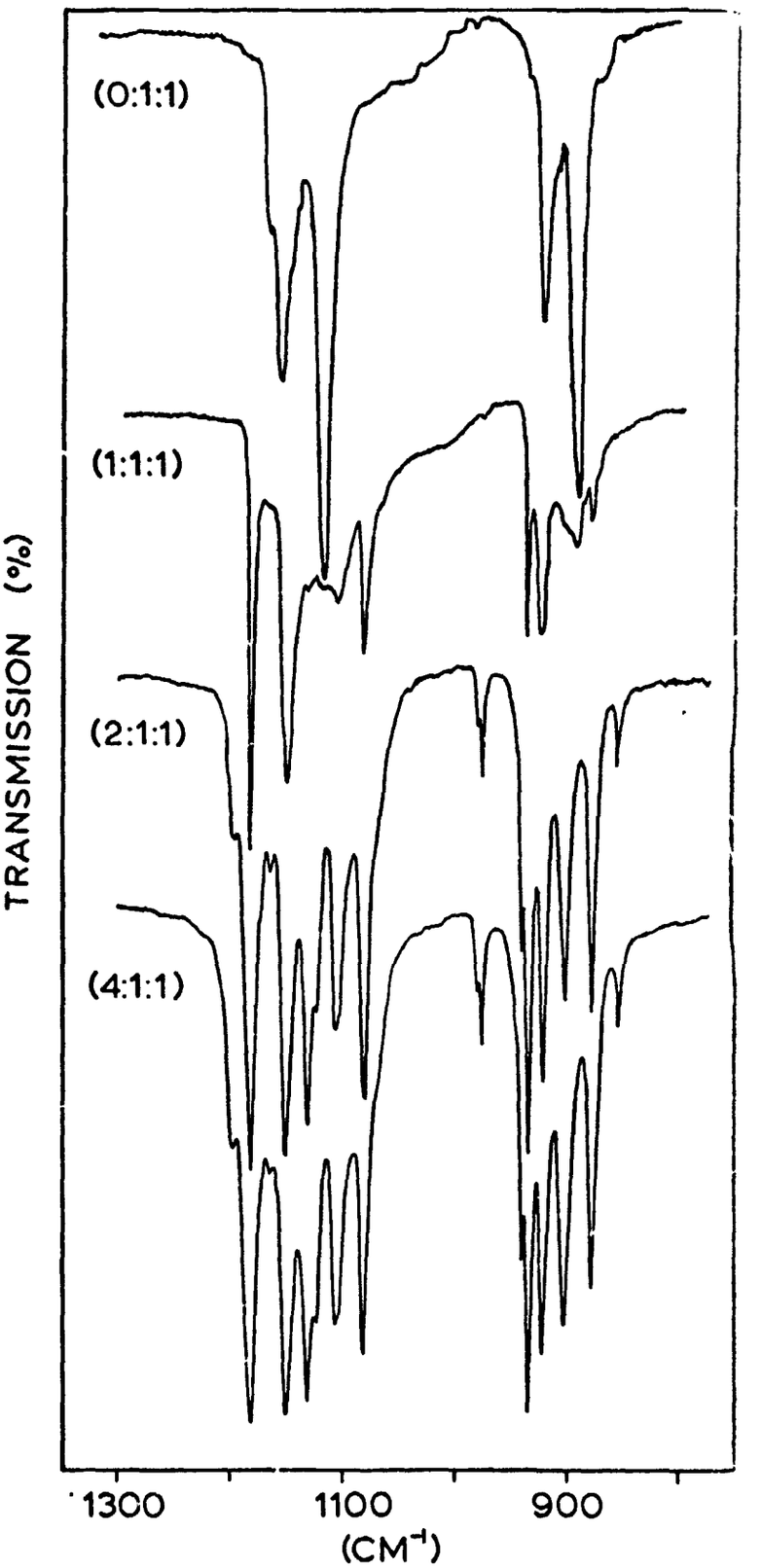

FIGURE 2

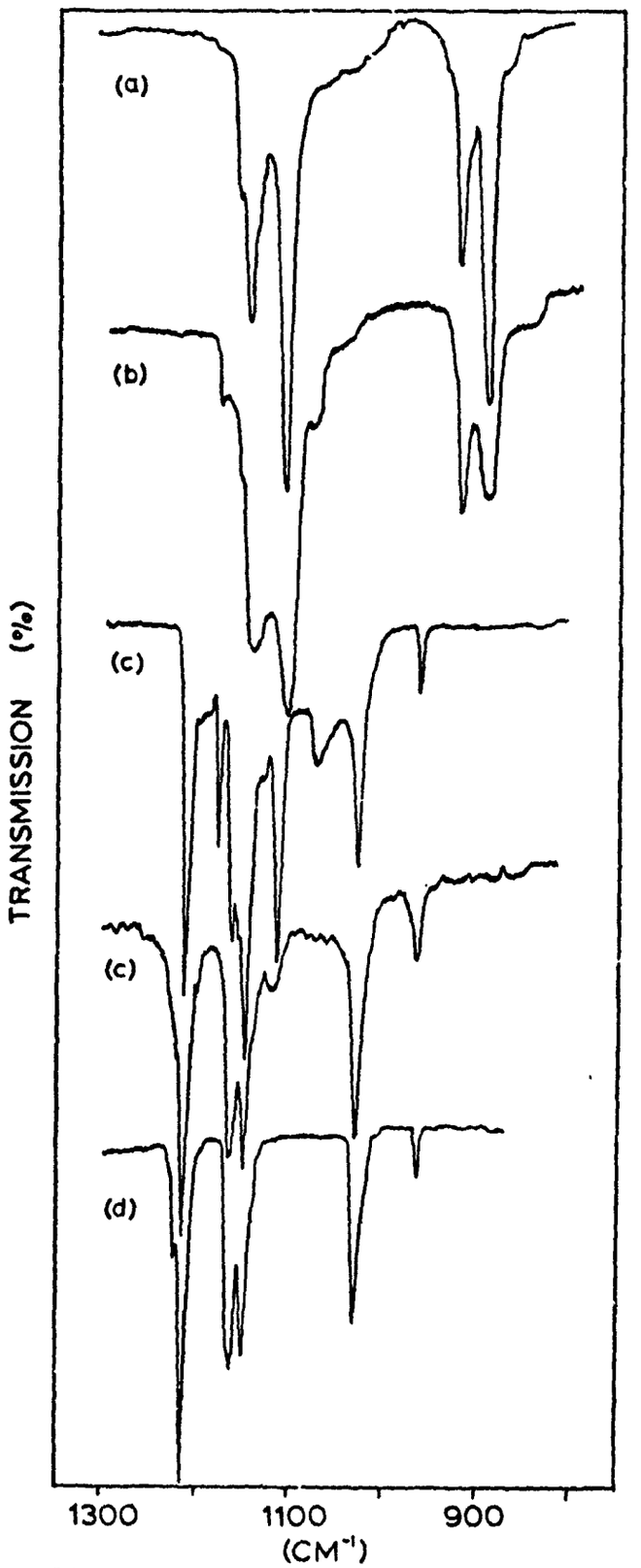

FIGURE 5

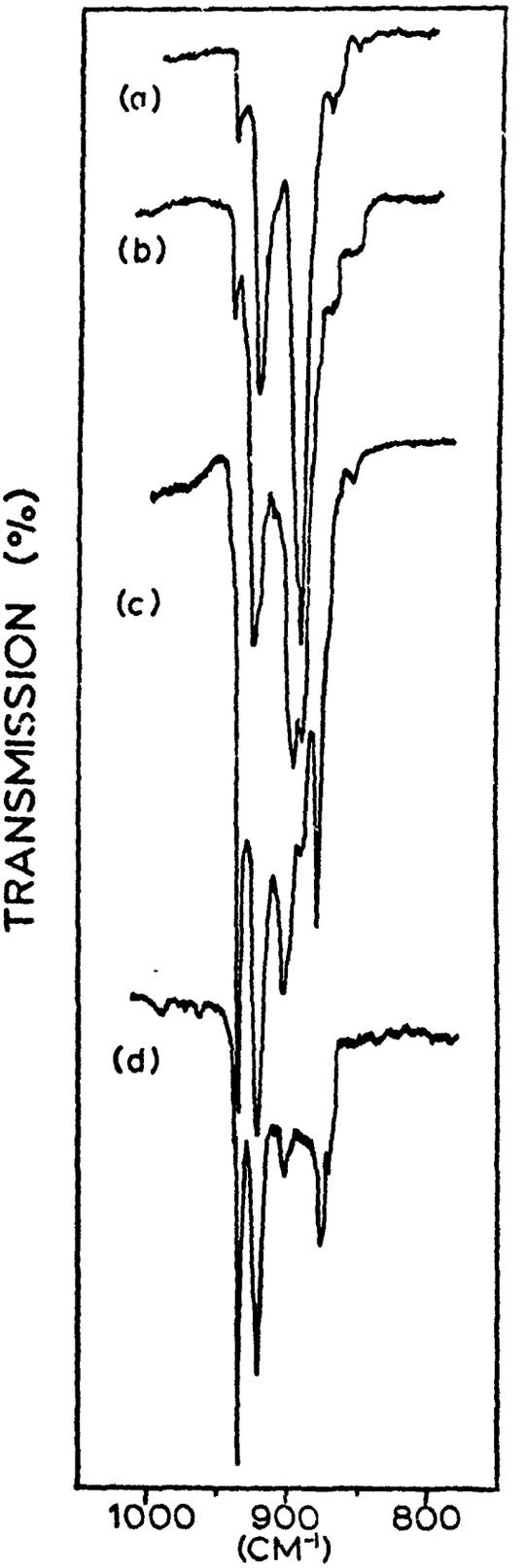

FIGURE 4

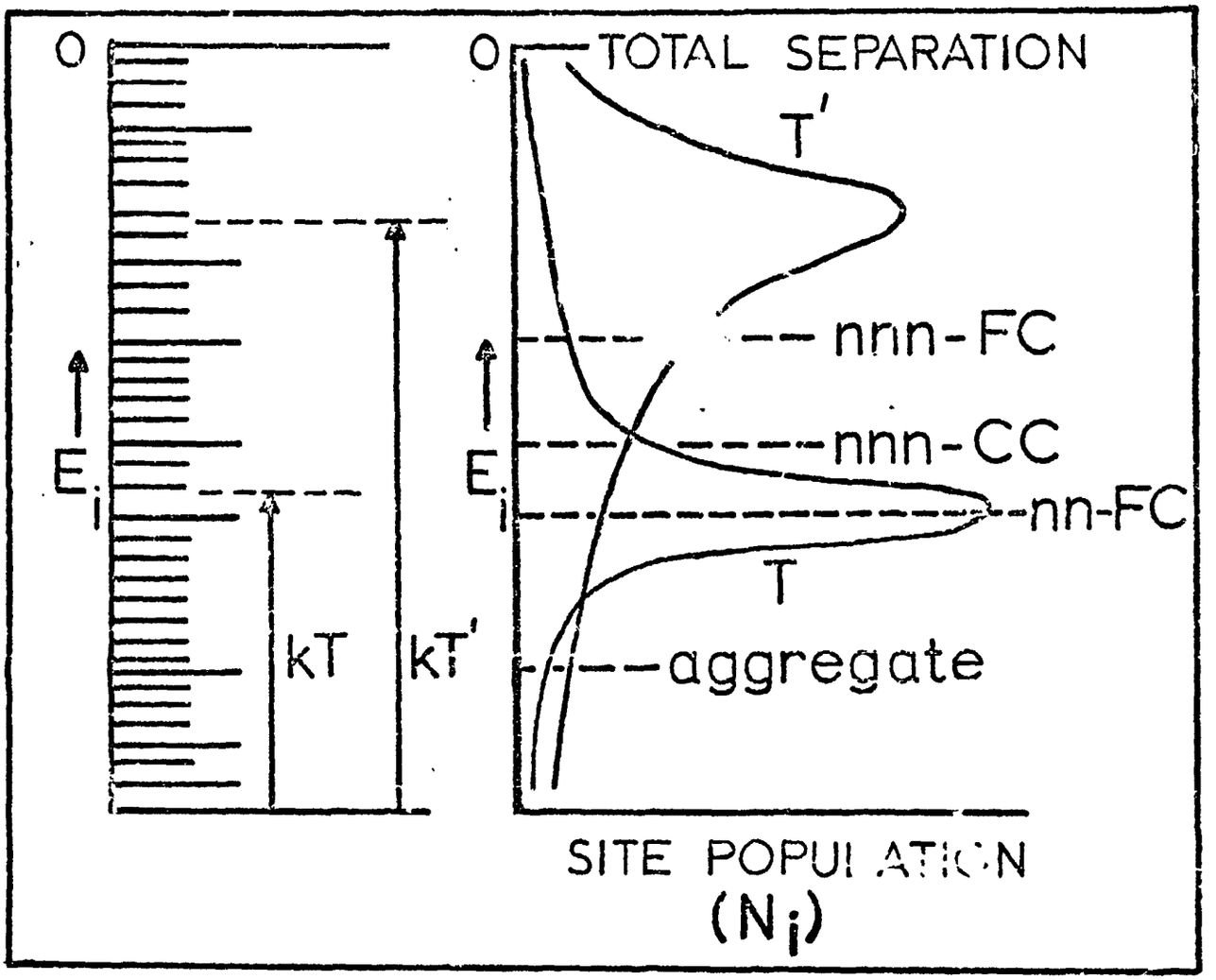
0
E_i
kT
kT'
0
TOTAL SEPARATION
T'
nnn-FC
nnn-CC
E_i
nn-FC
T
aggregate
SITE POPULATION
(N_i)

FIGURE 6